

# Simulations of ice-ocean dynamics in the Weddell Sea. Part II: Interannual variability 1985 — 1993

R. Timmermann, H.H. Hellmer, A. Beckmann

Alfred Wegener Institute for Polar and Marine Research, Germany

Short title:

**Abstract.** Investigations of sea ice-ocean interaction on the continental shelf in the southwestern Weddell Sea reveal a strong correlation between fluctuations of atmospheric forcing and the variability of sea ice formation. Anomalies of meridional wind stress in the inner Weddell Sea are consistent with the phase of the Antarctic Circumpolar Wave (ACW). Positive anomalies of northward wind stress cause an increase of sea ice export in the same, and of sea ice formation in the following year leading to an increased production of High Salinity Shelf Water. Driven by a varying zonal density distribution over the continental shelf, the circulation in the Filchner-Ronne Ice Shelf cavity fluctuates between two modes, each of which features a characteristic distribution of basal freezing and melting regions. Thus, signals of interannual atmospheric variability propagate into the deep ocean and the sub-ice shelf cavities.

# 1. Introduction

Water mass transformation in the Weddell Sea is strongly influenced by ice-ocean interaction. Intense cooling and brine release during sea ice formation on the southwestern continental shelf lead to an increase in surface water density, deep convection and thus to the formation of High Salinity Shelf Water (HSSW), one ingredient for the formation of Weddell Sea Bottom Water (WSBW) [*Foster and Carmack, 1976*]. An alternative way of WSBW formation is provided by mixing of Warm Deep Water (WDW) with Ice Shelf Water (ISW) which pours out of the Filchner-Ronne ice shelf cavity and sinks down on the continental slope [*Foldvik et al., 1985*]. This paper aims at an investigation of the seasonal and interannual variability of the coupled ice-ocean system and its response to atmospheric anomalies.

One of the prominent signals of variability in the Southern Ocean is the Antarctic Circumpolar Wave (ACW) [*White and Peterson, 1996*]. Based on an analysis of ECMWF reanalysis data along 56°S and of remote sensing sea ice concentration data, the ACW has been described as a set of closely connected anomalies of sea surface pressure and temperature, meridional wind stress and sea ice extent around Antarctica.

Further examination of the ECMWF reanalysis dataset, however, reveals an ACW-related oscillation also in the inner Weddell Sea, i.e. the region south of the line Kapp Norvegia - Joinville Island. Three month running means and especially annual means of meridional wind speed (Fig. 1) show periodic fluctuations which are in phase with the ACW. Maxima of northward wind stress found in 1988 and 1992, minima in 1986 and 1990; with 1990 being a year with an annual mean southward wind stress.

This oscillation is partly reflected by the area-averaged 2 m-air temperature (Fig. 2); southward and northward anomalies of meridional wind stress in 1990 and 1992 are linked to warm and cold anomalies of near surface temperature, respectively. The minimum of northward wind stress in 1986 and the subsequent maximum in 1988, however, are not reflected by anomalies of 2 m-temperature, corresponding to the analyses of *White and Peterson [1996]*, in which anomalies of 1986/1988 are less pronounced than in the years from 1990 onwards. Thus, the Antarctic Circumpolar Wave is not an ideally periodic system; the 4 years period is superimposed by additional fluctuations. In this paper we will investigate effects of ACW-related atmospheric variability on sea ice formation and water mass production in the inner Weddell Sea.

## 2. The Model

To achieve a consistent representation of both ice and ocean dynamics (including the ice shelves) we use the coupled ice-ocean model BRIOS-2 as presented by *Timmermann et al.* [this issue]. With a grid focussed on the Weddell Sector of the Southern Ocean, this model provides a reasonably fine horizontal resolution of 20 to 50 km in the area of our main interest. The s-coordinate ensures a high vertical resolution on the continental shelf and consideration of the major ice shelves provides an adequate representation of sub-ice shelf processes and their impact on the hydrography of the Weddell Sea.

## 3. Variability of sea ice-ocean interaction

### 3.1. Sea ice formation and export

Time series of the fresh water flux caused by sea ice formation in the inner Weddell Sea reveal a pronounced seasonal cycle of freezing and melting (Fig. 3). Typical maxima of monthly mean fresh water export or input are 200-300 mSv ( $1 \text{ mSv} = 10^3 \text{ m}^3 \text{ s}^{-1}$ ). The annual averages range from 18 to 59 mSv, with a nine-year mean of 33.7 mSv [*Timmermann et al.*, 2000]. Thus, roughly  $10^{12} \text{ m}^3/\text{a}$  of fresh water are extracted from the inner Weddell Sea and exported across the line Kapp Norvegia - Joinville Island. Time series of monthly mean fresh water export (Fig. 4) show a seasonal cycle which is quite similar to the sea ice production (Fig. 3). Compared to sea ice production, the maxima of ice export are shifted by a few weeks. As sea ice can be deformed or piled up by dynamic effects, ice export occurs intermittently, driven by synoptic wind variability.

Unlike the time series of *monthly* means, the correlation between *annual* means of ice production and export is not obvious; specifically, effects of ice production anomalies on ice export anomalies in the same or the following year are not discernable.

In contrast to that, a relation between ice export, and the sea ice production in the following year can easily be found. After the strong ice export in 1992 a positive anomaly of sea ice formation in 1993 is notable - an anomalous low ice coverage on the southwestern continental shelf during February/March 1993 is found both in the model and in the observations allowing the formation of large amounts of sea ice with the onset of autumn. This event is consistent with the phase of the ACW: Winter 1992 features a positive anomaly of meridional (northward) wind in the inner Weddell Sea (Fig. 1). Similar to that, albeit not as pronounced, is the correlation between the positive ice export anomalies of 1987

and sea ice formation in 1988; however these events appear not to be linked to the phase of the ACW.

*Comiso und Gordon* [1998] demonstrated that at least for the period 1979-1995 positive anomalies of winter ice extent in the Atlantic Sector of the Southern Ocean were succeeded by negative anomalies of summer sea ice extent and vice versa. This indicates that maxima of ice extent are not produced by a higher ice volume but by an increased sea ice export out of the inner Weddell Sea which is balanced by enhanced sea ice production in the subsequent year.

The sea ice export minimum in the simulation of 1990 is consistent with an annual mean southward wind stress over the inner Weddell Sea (Fig. 1). Sea ice formation in this region appears not be affected; however, we will demonstrate below how this event affects the fresh water flux and water mass formation over the continental shelf.

### Comparison to observations

Looking at the volume flux of sea ice (not shown) instead of the sea ice-related fresh water export reveals a time series quite similar to Fig. 4. The nine year mean simulated ice volume transport amounts to  $(42 \pm 26) \cdot 10^3 \text{ m}^3 \text{ s}^{-1}$  which is close to the estimated  $(46 \pm 8) \cdot 10^3 \text{ m}^3 \text{ s}^{-1}$  of *Harms et al.* [2000], derived from ULS measurements. So, model results and observations are in the same order of magnitude. Uncertainties in the assumptions of both our model and the observations, however, exclude a good agreement between the individual annual means of both time series.

### 3.2. Water Mass Formation

*Timmermann et al.* [2000] discussed the simulated water mass structure of the Weddell Sea in the 9-year mean. Comparing the climatological monthly means of March and September (Fig. 5 a, b) one notices only a small variability. A pronounced seasonal cycle can be seen in the temperature of the light, near-surface water masses ( $S < 34.4$ ) in the central Weddell Sea. However, variations in properties of the denser, saline water on the continental shelf are small. In this region, the water column is covered by sea ice for most of the year; the ice-free period in summer is too short to provide much of a warming. Relatively stable stratification in summer reduces vertical mixing and the input of ice shelf water (ISW) from the sub-ice shelf cavities provides an additional cooling.

High Salinity Shelf Water (HSSW) with  $S > 34.75$  is poorly represented in the nine-year mean and even in the climatological seasonal cycle (Fig. 5 a, b). Analysis of individual monthly means, however, indicates that the interannual variability of shelf water mass properties is significantly higher than the

seasonal. A time series of the simulated volume of HSSW (Fig. 6) reveals a pronounced seasonal cycle minted by the freezing and melting of sea ice in the southwestern Weddell Sea. However, HSSW is almost absent from late 1989 until the winter of 1992. The change in shelf water mass structure is illustrated by the  $\Theta$ - $S$ -diagrams of August 1991 and August 1992 (Fig. 5 c, d): While in the winter of 1991 no water with salinity exceeding 34.67 exists, a relatively large amount of High Salinity Shelf Water with salinity up to 34.85 has been formed one year later.

A time series of the ocean surface fresh water flux on the continental shelf (Fig. 7) indicates the role of sea ice in this variability. In the 9-year average, 15 mSv of fresh water are extracted from the water column on the continental shelf. The seasonal cycle of freezing and melting is well pronounced, modulated by a distinguished interannual variability. For the period 1985 through 1989, the time series features a quasi-stationary seasonal cycle with a rather constant amplitude. The water mass structure in this period is very much resembled by the  $\Theta$ - $S$ -diagrams in Fig. 5 a, b.

The situation changes drastically with the strong southward wind stress anomaly found in 1990 (Fig. 1) which leads to a pronounced ice export minimum (Fig. 4). Sea ice formed on the continental shelf is unable to leave the area northward, so that further sea ice formation is strongly reduced. Sea ice coverage during the summer minimum 1990/91 remains high — both in remote sensing observations [Heygster *et al.*, 1996] and in the model simulation. At the end, winter sea ice formation and thus fresh water extract in the simulated years 1990-1991 is greatly reduced (Fig. 7). In this period, High Salinity Shelf Water vanishes from the continental shelf and is replaced by water which is too light to contribute to the formation of Weddell Sea Bottom Water (Fig. 5 c).

In contrast, 1992 is characterized by a maximum of northward wind stress (Fig. 1) which is linked to a positive anomaly of sea ice export. Increased sea ice formation in this and the subsequent winter provides enough salt input to replenish the HSSW (Fig. 5 d) with salinities exceeding 34.8. Hence, water mass structure approaches the climatological mean (Fig. 5 a, b) again.

In reality, part of the newly formed saline water would spread into the deep ocean and contribute to the formation of WSBW. This spreading occurs mainly through isolated *plumes* which are guided by deep ocean ridges or canyons [Jungclauss und Backhaus, 1994; Jungclauss *et al.*, 1995] and have a typical horizontal scale of a few kilometers [Baines und Condie, 1998]. Like every hydrostatic coarse resolution model, BRIOS-2 is not able to resolve these processes and overestimates mixing with ambient water masses. Thus, density is reduced to a point which makes it impossible to sink down to the abyss; instead, these waters enter the Weddell Sea circulation at the WSDW level.

Another portion of the saline water leaves the continental shelf and spreads northward along the western continental slope [Muench and Gordon, 1995]. In the BRIOS-2 simulations, cold, saline anomalies can be traced along the continental slope in the western Weddell Sea. About 12 month after their formation these anomalies reach the tip of the Antarctic Peninsula and leave the Weddell basin through gaps in the South Scotia Arc. Thus, surface forcing anomalies due to the ACW and their response in the Weddell Sea’s outflow properties are correlated with a time lag of roughly two years, half the ACW period.

The remaining question is, why a relation between ACW and bottom water production is significant only for 1990–1993, but not for the period 1985–1989. As shown in the introduction, anomalies of near-surface air temperature correlate with meridional wind fluctuations only for the period 1990–1993. In contrast to 1992, the positive meridional wind stress anomaly of 1988 is not linked to a cold anomaly of the 2 m-temperature. Comparing monthly and annual means (Fig. 2) shows that the 2 m-temperature’s interannual variability is determined by variations of the mean winter temperature. While 1992 can be classified as an extremely cold winter, the winter of 1988 is specified relatively warm. Therefore, compared to 1992, sea ice formation and export in 1988 are reduced.

In addition to that, the negative anomalies of northward wind stress differ in magnitude. In 1986, the annual mean wind stress is still northward, while in 1990 the annual mean is directed southward. The latter is clearly visible in the winter months of 1990 (Fig. 1, top) and is responsible for the unusually low sea ice export in 1990 and the reduced sea ice formation in the following year.

In summary, the period 1990–1993 differs from the years 1985–1989 by higher extrema, causing more pronounced anomalies in sea ice formation and water mass production on the continental shelf.<sup>1</sup> However, it should be kept in mind that the ECMWF reanalysis data used to force the simulation are a model output themselves. In the framework of this study we are unable to distinguish whether the differences between the two periods 1985–1989 and 1990–1993 are realistic or just due to an insufficient data coverage in the earlier years. So, the results we presented are not meant to be a hindcast of the Weddell Sea’s state in the years 1985 through 1993; instead, they are supposed to illustrate how the coupled ice ocean system reacts on different modes of atmospheric forcing.

---

<sup>1</sup>An alternate hypothesis, that in our simulation the ACW ran ”out of phase“ by repeating a nine-year period of forcing data, was rejected after a series of experiments omitting the data from 1985 had produced the same results.

## 4. Ice Shelf-Ocean Interaction

Models of ice shelf-ocean interaction [e.g., *Hellmer und Ollers, 1989; Jenkins, 1991; Gerdes et al., 1999*] indicate that ice shelf-ocean interaction is dominated by the pressure-dependence of the *in situ*-freezing point of sea water. Typically, large areas of basal melting are found near the grounding line where the *in situ*-freezing temperature is significantly lower than the surface freezing point. In regions with flow in the direction of decreasing ice shelf thickness, ice crystals can accumulate at the ice shelf base and form large bodies of marine ice [*Engelhardt und Determann, 1987*].

Corresponding to that, the modeled Filchner-Ronne sub-ice shelf circulation in BRIOS-2 induces the formation of large areas of basal melting, especially near the grounding line. North of the combined Henry/Korff Ice Rise complex the long-term mean features a region of basal freezing of up to 30 cm marine ice per year [*Timmermann et al., 2000*]. Area-averaged basal melting amounts to 29.8 cm/yr.

Analysing individual monthly means of sub-ice shelf basal mass fluxes and ocean circulation, we found that the cavity beneath the Filchner-Ronne Ice Shelf is not an independent system but is greatly influenced by processes on the continental shelf north of the ice shelf edge. Sea ice plays an important part in this closely coupled system, as its formation determines the density distribution on the southwestern continental shelf.

From May to October, during the months of intense sea ice formation, dense, saline water is formed on the continental shelf, portions of it penetrating into the sub-ice shelf cavity. Depending on where the densest water is located on the continental shelf, the simulated sub-ice shelf circulation fluctuates between two modes:

The first mode (Fig. 8, top) is characterized by the density maximum located on the western Weddell shelf, near the Antarctic Peninsula. In this case, water from the open ocean penetrates through the Ronne Depression into the FRIS cavity leading to high melting rates at the base of the western Ronne Ice Shelf. Driven by the density gradient along the ice shelf edge, an anticyclonic circulation develops in the Ronne cavity and around Berkner Island. In the Filchner cavity, a weak cyclonic circulation exists which transports Ice Shelf Water northward along the east coast of Berkner Island, i.e., on the western slope of the Filchner Trough. This leads to basal freezing at the northwestern edge of Filchner Ice Shelf, in agreement with observations and previous modeling [*Grosfeld et al., 1998*]. The accumulation is subject to a pronounced interannual variability with basal freezing rates around 1.5 m/yr in years with low HSSW formation.

The circulation is reversed for density maximum situated north of Berkner Island, which is typical

for years with a high formation rate of HSSW (Fig. 8, bottom). In this mode, shelf water masses flow into the cavity directly west and east of Berkner Island. Thus, the highest melting rates are found west of Berkner Island and over the Filchner Trough. An anticyclonic circulation with a vertically integrated transport of up to 2.5 Sv develops in the Filchner Trough, while a cyclonic circulation dominates beneath the Ronne Ice Shelf. Melting rates at the Filchner Ice Shelf base reach up to 2.5 m/yr while they do not exceed 1.5 m/yr in the "low HSSW"-situation.

The FRIS cavity simulations of *Gerdes et al.* [1999], forced with constant prescribed boundary conditions, feature a distribution of freezing and melting regions which is similar to our "low HSSW"-situation. One of the differences to our experiments is a stronger cyclonic circulation in the Filchner Trough, which enhances the region of basal freezing in the northwestern corner of the Filchner Ice Shelf. Another one is that the zone of high melting rates beneath the central Filchner Ice Shelf is missing which is more pronounced in years with a high formation rate of HSSW but is also present in the "low HSSW"-case.

Apparently, the circulation in the FRIS cavity changes as part of an interannual variability, driven by fluctuations of density (salinity) distribution on the continental shelf north of the ice shelf edge. From analysis of water mass properties, *Nøst und Foldvik* [1994] concluded that south of Berkner Island water is transported from the Ronne into the Filchner cavity. However, *Hellmer und Olbers* [1991] already showed that the direction of flow south of Berkner Island depends on the density distribution north of the ice shelf edge with a flow from the Ronne into the Filchner cavity in the case of high density water in the Ronne Depression. In BRIOS-2, this situation is typical for the years 1986 to 1989. During the period of low salt input on the continental shelf (1990/91) flow across the ice shelf edge is rather weak and distinct circulation patterns are hardly visible. During the period of high salt input, especially in the winter of 1992, a cyclonic circulation around Berkner Island with a transport from the Filchner into the Ronne cavity develops. The local wind field north of the ice shelf edge does not seem to play a major role in this process: a significant correlation between the wind direction and the sub-ice shelf circulation was not found.

In an earlier BRIOS study *Beckmann et al.* [1999], the change from a cyclonic to an anticyclonic circulation in the Filchner Trough was described as a seasonal signal in a standalone ocean-ice shelf model (BRIOS-1). However, BRIOS-1 was forced by quasi-climatological monthly means (no interannual variability), which were repeated for each year of integration. Forcing data were derived from the integration of a standalone sea ice model (BRIOS-0) which was forced the same way as the coupled ice-ocean model BRIOS-2 (see *Beckmann et al.*, [1999] for further details). Similar to the

results presented here, net freezing rates and thus salt input north of Berkner Island in BRIOS-0 is high in the winter months of 1992 and 1993. This signal is still present in the climatological monthly means, so that BRIOS-1, forced with these data, reproduces an interannual variability as part of the seasonal cycle. If, as in BRIOS-2, the interannual variability of atmospheric boundary conditions is properly taken into account, seasonal variations of the sub-ice shelf circulation are much smaller than the differences between the individual years of simulation.

## 5. Variability of the fresh water balance of the inner Weddell Sea

According to the analyses of *Timmermann et al.* [2000], the fresh water budget of the inner Weddell Sea can be described as a long-term balance of fresh water loss due to sea ice formation and export and fresh water gain due to precipitation and ice shelf melting. Time series of monthly and annual means of each component (Fig. 9) indicate that the long-term balance is the residuum of high numbers different in sign. The seasonal and interannual variability of the surface fresh water budget is dominated by fluctuations of sea ice formation both on a seasonal and interannual time scale: In years with only moderate sea ice formation, the surface fresh water budget is balanced or even positive. If sea ice formation is strong (1987, 1988 or 1993), however, an annual mean of up to 31 mSv of fresh water is extracted from the surface of the inner Weddell Sea. These fluctuations in the annual mean fresh water budget add up to a standard deviation of 13 mSv which is considerably larger than the nine-year mean of 5.3 mSv [*Timmermann et al.*, 2000]. Therefore, the net southward advection of salt into the inner Weddell Sea is not significantly different from zero.

Compared to the fluctuations in sea ice formation, the variability of sub-ice shelf melting (Fig. 10) is small. Beneath the Eastern Weddell Ice Shelves, relatively warm water from the coastal current is in direct contact with the ice shelf base. Due to high flushing rates, variations of the water mass properties in the coastal current are advected into the cavity causing a high variability of EWIS basal melt rates. Striking are the high melting rates in the first quarter of 1986, 1990 and 1993, which are also found in the basal melt rates of LIS and FRIS. These anomalies are caused by a very small summer ice extent in 1986 and 1993, which can be found both in the model and in the observations [*Hegster et al.*, 1996]. In 1990, relatively large areas of the Weddell Sea remain ice covered, but the simulation features open water along the eastern Weddell Sea coast and low ice concentration off Filchner-Ronne and Larsen ice shelves. In these regions, the ocean surface temperature increases by absorption of solar radiation.

Downwelling transports this signal across the pycnocline and eventually it is advected into the sub-ice shelf cavity where it leads to an enhanced basal melting.

Similar to that, we have shown that variations of water mass properties on the southwestern continental shelf affect the sub-ice shelf circulation of FRIS. During the period of vanishing HSSW (1990/91) fresh water input by basal melting is reduced from typical values around 4 mSv to less than 2 mSv. Variability of monthly means is quite low during this period. Water mass exchange across the ice shelf edge is reduced, so that sub-ice shelf circulation and the ice-ocean interaction are virtually decoupled from varying boundary conditions at the ice shelf edge. With the formation of new HSSW, starting in 1992, the flow into the cavity increases and basal melting recovers. The reversal of sub-ice shelf circulation, however, has no significant impact on the area-averaged basal melt rates.

## 6. Conclusions

Simulations with the coupled ice-ocean model BRIOS-2 indicate that large scale atmospheric oscillations have a strong influence on bottom water production in the Weddell Sea. Anomalies of meridional wind stress which are part of the Antarctic Circumpolar Wave (ACW) cause significant fluctuations of the sea ice export across the line Kapp Norvegia — Joinville Island. Negative (i.e., southward) wind stress anomalies are related to ice export minima and lead to reduced sea ice formation and bottom water production on the southwestern continental shelf. Positive anomalies of meridional (northward) wind stress, in turn, cause an enhanced ice export, resulting in a reduced summer sea ice coverage followed by stronger sea ice formation in the subsequent winter. High Salinity Shelf Water (HSSW) which is formed during these periods mixes with Modified Circumpolar Deep Water and is transported northward along the western continental slope. Portions of this water can be traced as cold, saline anomalies which reach the tip of the Antarctic Peninsula roughly 12 months after their formation. Given a four year period of the ACW, wind stress anomalies and the response in the Weddell Sea outflow are phase shifted by roughly half the ACW's period.

We have also demonstrated that sea ice formation on the southwestern continental shelf affects the ocean circulation in the Filchner-Ronne ice shelf cavity significantly. An anticyclonic circulation in the Ronne cavity and around Berkner Island is the common situation if the maximum of shelf water density is found on the western edge of the continental shelf. However, strong sea ice formation in the southwestern Weddell Sea leads to a salt enrichment particularly on the Berkner Bank. With the density maximum to be found north of Berkner Island, sub ice-shelf circulation reverses to an

anticyclonic circulation in the Filchner Trough and a cyclonic circulation beneath the Ronne Ice Shelf; however, area-averaged basal melt rates are hardly affected. Hence, by affecting sea ice formation and thus the density distribution of the continental shelf, signals of atmospheric variability propagate both into the deep ocean and into the sub-ice shelf cavities.

## Acknowledgements

The authors would like to thank W. Cohrs and C. Lichey for preparing the ECMWF and NCEP atmospheric forcing fields which were received via the German Weather Service (Deutscher Wetterdienst, DWD) and the NOAA-CIRES Climate Diagnostics Center, Boulder, using the website <http://www.cdc.noaa.gov/>, respectively. Helpful discussions with E. Fahrbach are gratefully acknowledged.

## References

- Baines, P. G., and S. Condie: Observations and modelling of Antarctic downslope flows: A review. In: *Ocean, Ice and Atmosphere: Interactions at the Antarctic Continental Margin. Antarct. Res. Ser.*, **75**, edited by S.S. Jacobs and R.F. Weiss, 29-49, AGU, Washington, D.C., 1998.
- Beckmann, A., H. H. Hellmer, and R. Timmermann: A numerical model of the Weddell Sea: large scale circulation and water mass distribution. *J. Geophys. Res.*, **104(C10)**, 23375-23391, 1999.
- Comiso, J. C., and A. L. Gordon: Interannual variability in summer sea ice minimum, coastal polynyas and bottom water formation in the Weddell Sea. In: *Antarctic Sea Ice: Physical Processes, Interactions and Variability, Antarctic Res. Ser.*, **74**, edited by M. O. Jeffries, 293-315, 1998.
- Engelhardt, H., and J. Determann: Borehole evidence for a thick layer of basal ice in the central Ronne Ice Shelf. *Nature*, **327(6120)**, 318-319, 1987.
- Foldvik, A., T. Gammelsrød, and T. Tørresen: Circulation and water masses on the southern Weddell Sea shelf. *Antarct. Res. Ser.*, **43**, edited by S. S. Jacobs, 5-20, AGU, Washington, D.C., 1985.
- Foster, T. D. , and E. C. Carmack: Frontal zone mixing and Antarctic Bottom Water formation in the southern Weddell Sea. *Deep Sea Res.*, **23(4)**, 301-317, 1976
- Gerdes, R., J. Determann , and K. Grosfeld: Ocean circulation beneath Filchner-Ronne Ice Shelf from three-dimensional model results. *J. Geophys. Res.*, **104(C7)**, 15827-15842, 1999.
- Grosfeld, K., H. H. Hellmer, M. Jonas, H. Sandhäger, M. Schulte , and D. G. Vaughan: Marine ice beneath Filchner Ice Shelf: Evidence from a multidisciplinary approach. In: *Ocean, Ice and Atmosphere: Interactions at the Continental Margin, Antarct. Res. Ser.*, **75**, edited by S. S. Jacobs , and R. F. Weiss, 319-339, AGU, Washington, D. C., 1998.
- Harms, S., E. Fahrbach , and V. H. Strass: Ice transport in the Wedell Sea. *J. Geophys. Res.*, (submitted), 2000.
- Hellmer, H. H., and D. Olbers: A two-dimensional model for the thermohaline circulation under an ice shelf. *Antarctic Science*, **1**, 325-336, 1989.
- Hellmer, H. H., and D. Olbers: On the thermohaline circulation beneath Filchner-Ronne Ice Shelf. *Antarctic Science*, **3(4)**, 433-442, 1991.
- Heygster, G., L. T. Pedersen, J. Turner, C. Thomas, T. Hunewinkel, H. Schottmüller, and T. Viehoff: PELICON: Project for estimation of long-term variability of ice concentration. *EC Contract Report EV5V-CT93-0268 (DG 12)*, Bremen, 1996.
- Jenkins, A.: A one-dimensional model of ice shelf-ocean interaction. *J. Geophys. Res.*, **96(C11)**, 20671-20677,1991.

- Jungclauss, J. H., and J. O. Backhaus: Application of a transient reduced gravity plume model to the Denmark Strait Overflow. *J. Geophys. Res.*, **99(C6)**, 12375-12396, 1994.
- Jungclauss, J. H., J. O. Backhaus, and H. Fohrmann: Outflow of dense water from the Storfjord in Svalbard: A numerical model study. *J. Geophys. Res.*, **100(C12)**, 24719-24728, 1995.
- Muench, R. D., and A. L. Gordon: Circulation and transport of water along the western Weddell Sea margin. *J. Geophys. Res.*, **100(C9)**, 18503-18515, 1995.
- Nøst, O. A., and A. Foldvik: A model of ice shelf-ocean interaction with application to the Filchner-Ronne and Ross Ice shelves. *J. Geophys. Res.*, **99(C7)**, 14243-14254, 1994
- Timmermann, R., A. Beckmann und H. H. Hellmer: The role of sea ice in the fresh water budget of the Weddell Sea. *Annals of Glaciology*, Vol. **33** (in press), 2000.
- White, B. W., and R. G. Peterson: An Antarctic circumpolar wave in surface pressure, wind, temperature and sea ice extent. *Nature*, **380(6576)**, 699-702, 1996.

---

Received \_\_\_\_\_

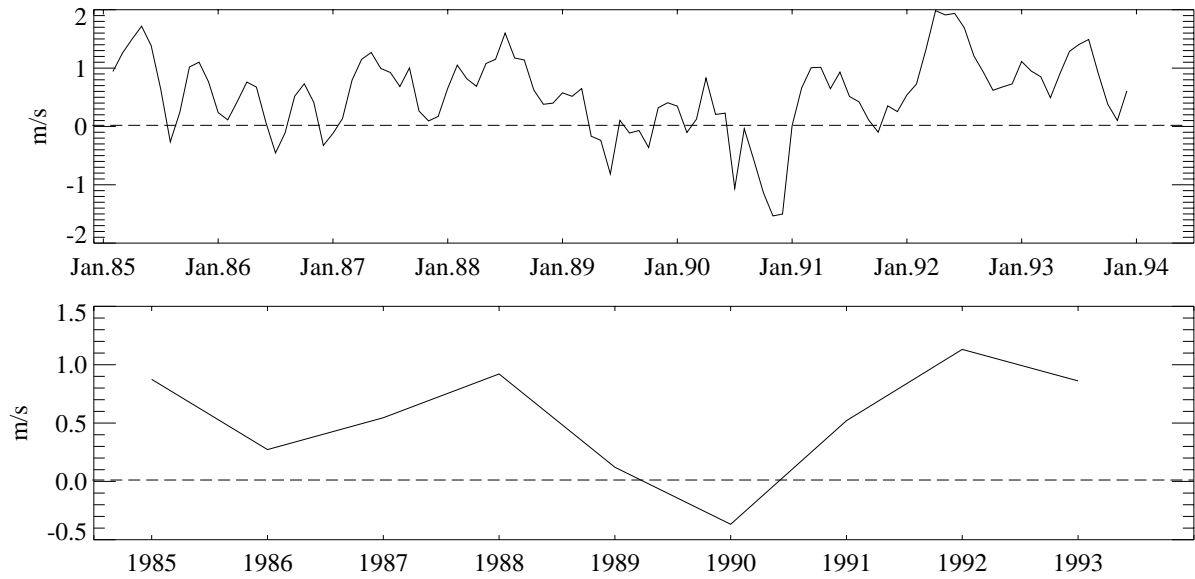


**Figure 1.** Three month running means (top) and annual means (bottom) of meridional (northward) 10 m-wind speed from the ECMWF reanalyses of 1985-1993, averaged over the inner Weddell Sea.

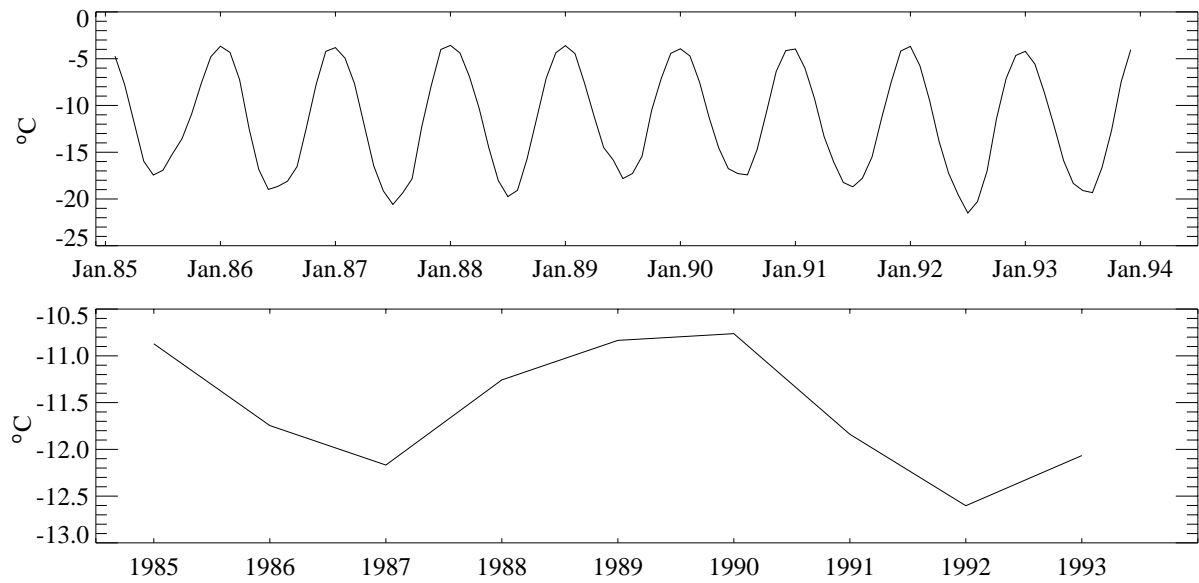


**Figure 2.** Three month running means (top) and annual means (bottom) of 2 m-temperature from the ECMWF reanalyses of 1985-1993, averaged over the inner Weddell Sea.

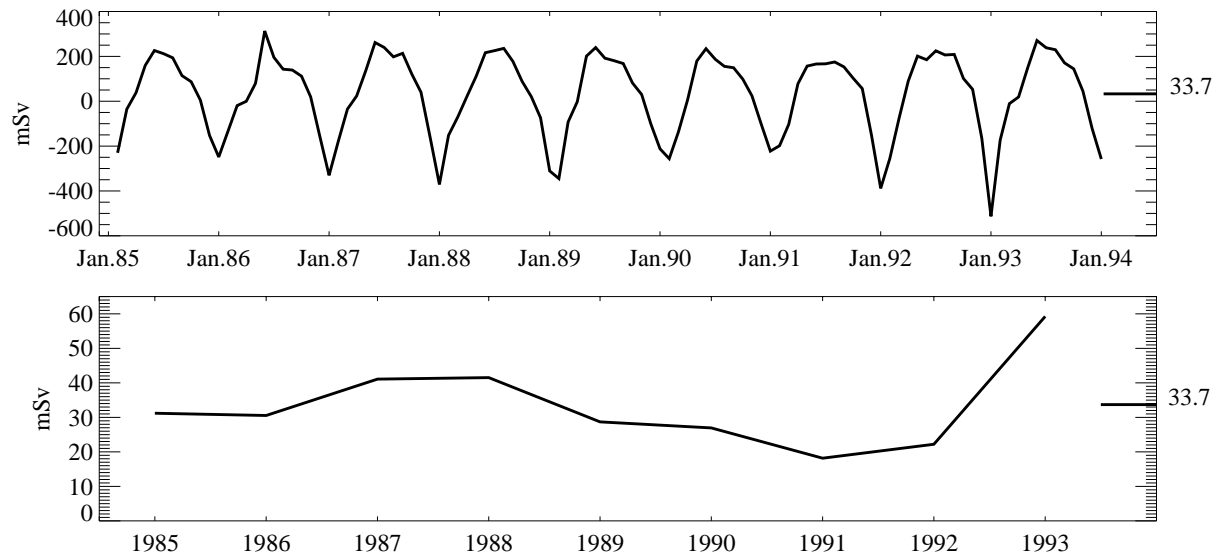


**Figure 3.** Monthly (top) and annual (bottom) means of the simulated sea ice related fresh water flux extracted from the inner Weddell Sea. Positive values indicate sea ice formation, i.e. loss of fresh water.

1 mSv =  $10^3 \text{ m}^3 \text{ s}^{-1}$ .

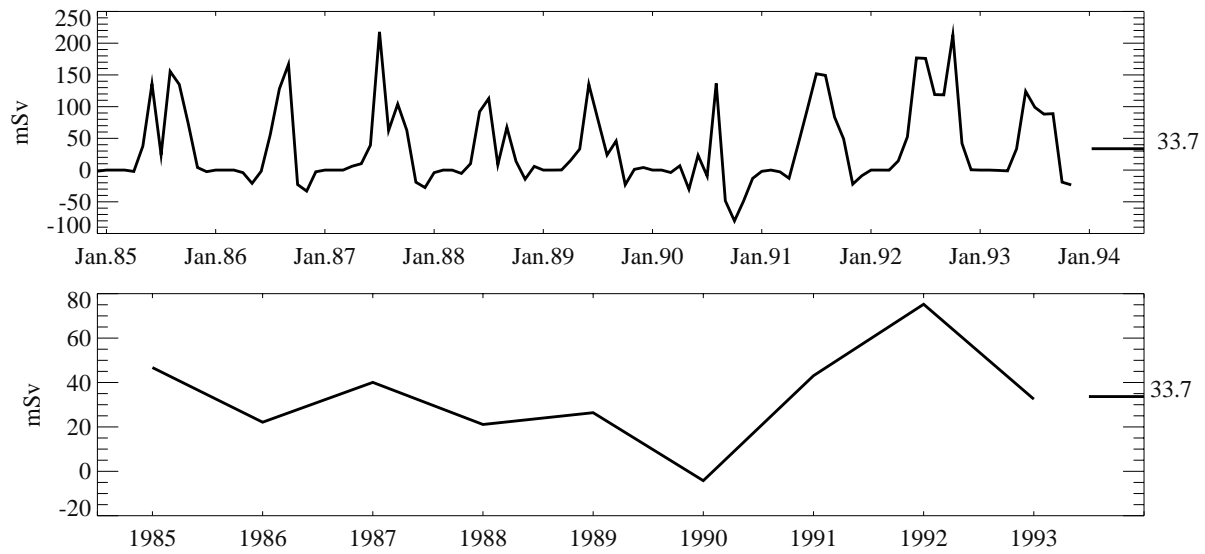


**Figure 4.** Monthly (top) and annual (bottom) means of the fresh water export due to the drift of sea ice and snow out of the inner Weddell Sea.

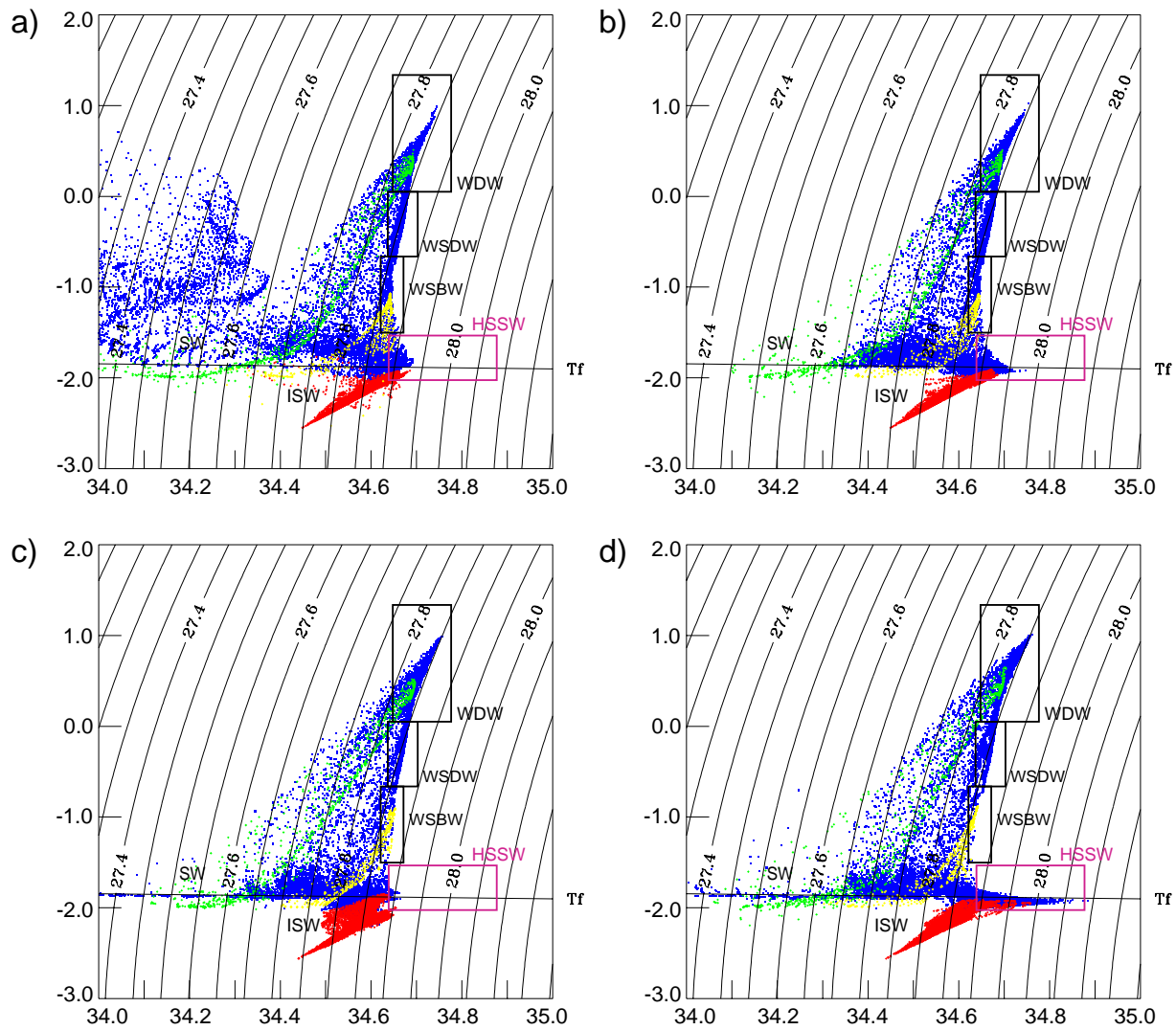


**Figure 5.** Simulated  $\Theta$ - $S$ -diagrams of the inner Weddell Sea, i.e., the region south of the Line Kapp Norvegia - Joinville Island as climatological monthly means of a) March and b) September and monthly means of c) August 1991 and d) August 1992. Properties are marked according to the locations of grid points, i.e. ocean (blue) and cavities of Filchner-Ronne Ice Shelf (FRIS, red), Larsen Ice Shelf (LIS, yellow) and the Eastern Weddell Ice Shelves (EWIS, green).

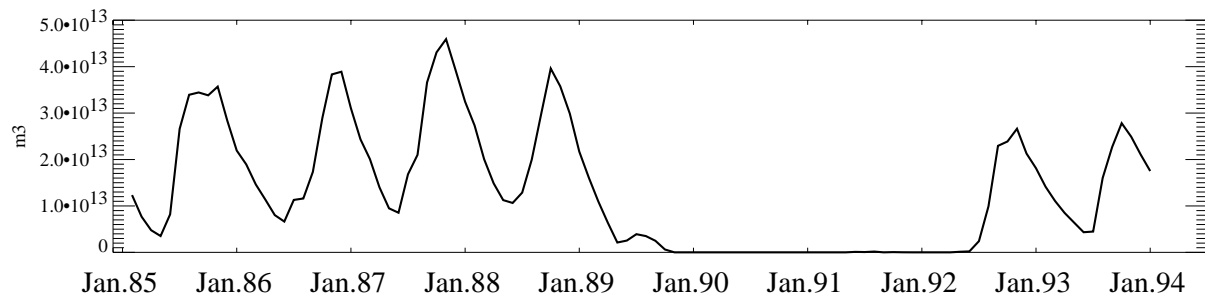


**Figure 6.** Time series of the simulated volume of saline shelf water, i.e., water with  $S > 34.65$  and  $-2^{\circ}\text{C} < \Theta < -1.6^{\circ}\text{C}$ .

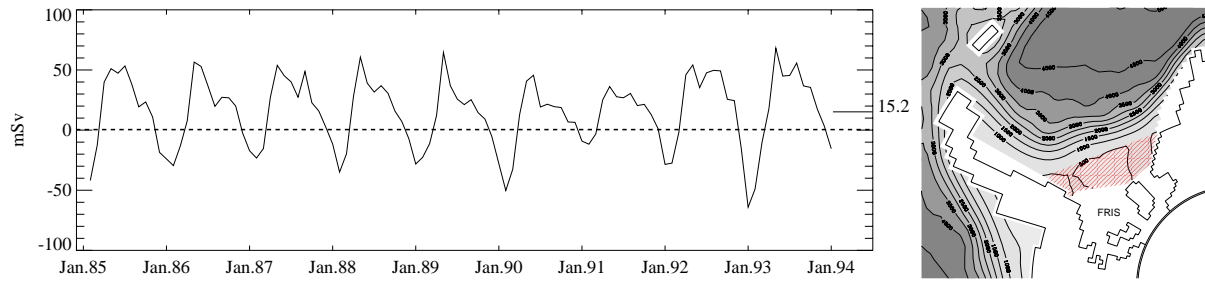


**Figure 7.** Time series of sea ice-related fresh water fluxes on the continental shelf (left), as marked by the shaded area on the contour plot of bottom topography (right).

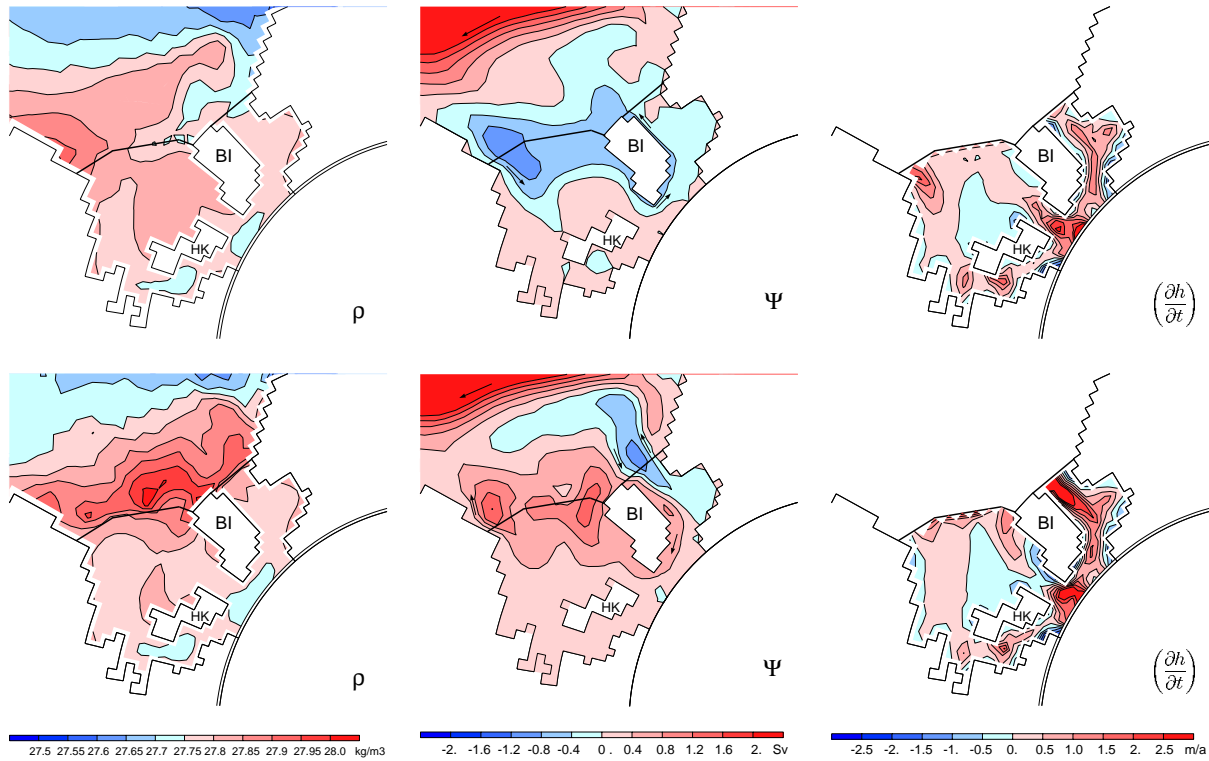


**Figure 8.** Characteristics of ice shelf-ocean interaction in situations with the maximum density located on the western edge of the continental shelf (September 1989, top) and north of Berkner Island (September 1992, bottom). Displayed are monthly mean surface density (left), vertically integrated transport (stream function  $\Psi$ , middle) and FRIS basal melting rates (right). Arrows indicate directions of the regional circulation. The bold black lines indicate the ice shelf edge. BI = Berkner Island, HK = Henry/Korff Ice Rise.

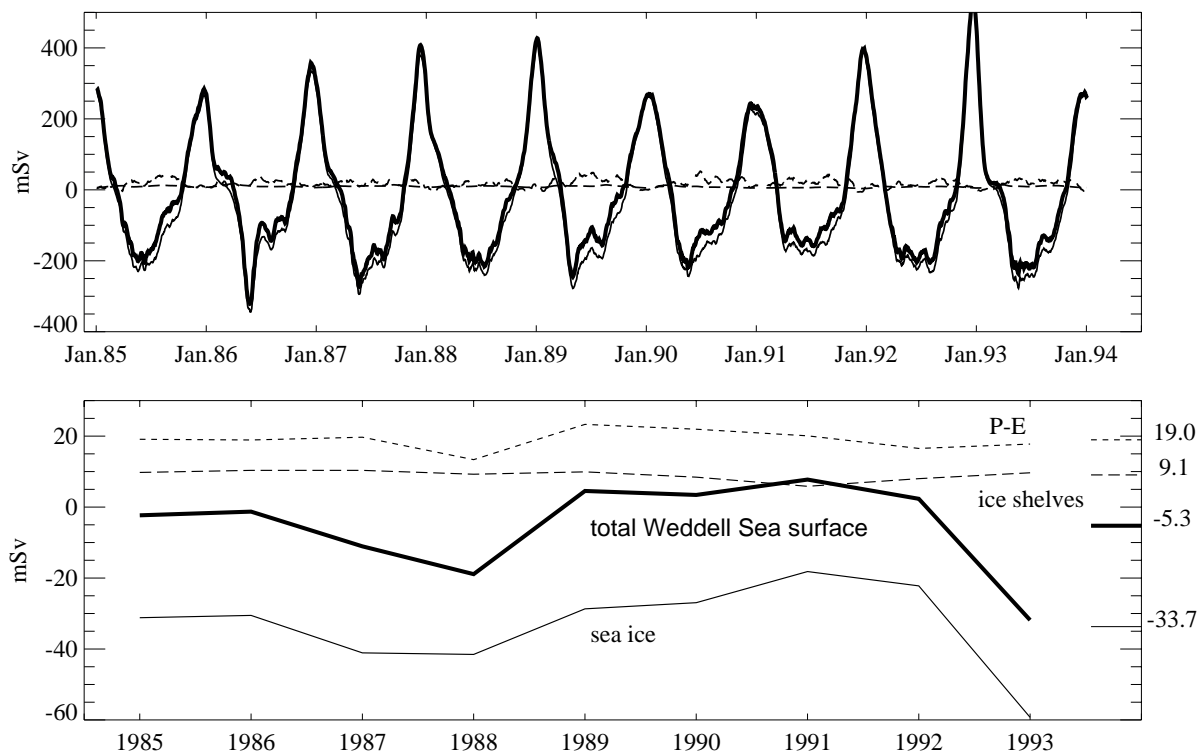


**Figure 9.** Time series of 30d running mean (top) and annual mean (bottom) fresh water fluxes from sea ice formation (solid), basal melting of ice shelves (dashed) and net precipitation (dotted) and the overall surface fresh water fluxes in the inner Weddell Sea (bold). Numbers at the right axis indicate the 9-year averages.  $1 \text{ mSv} = 10^3 \text{ m}^3/\text{s}$ .

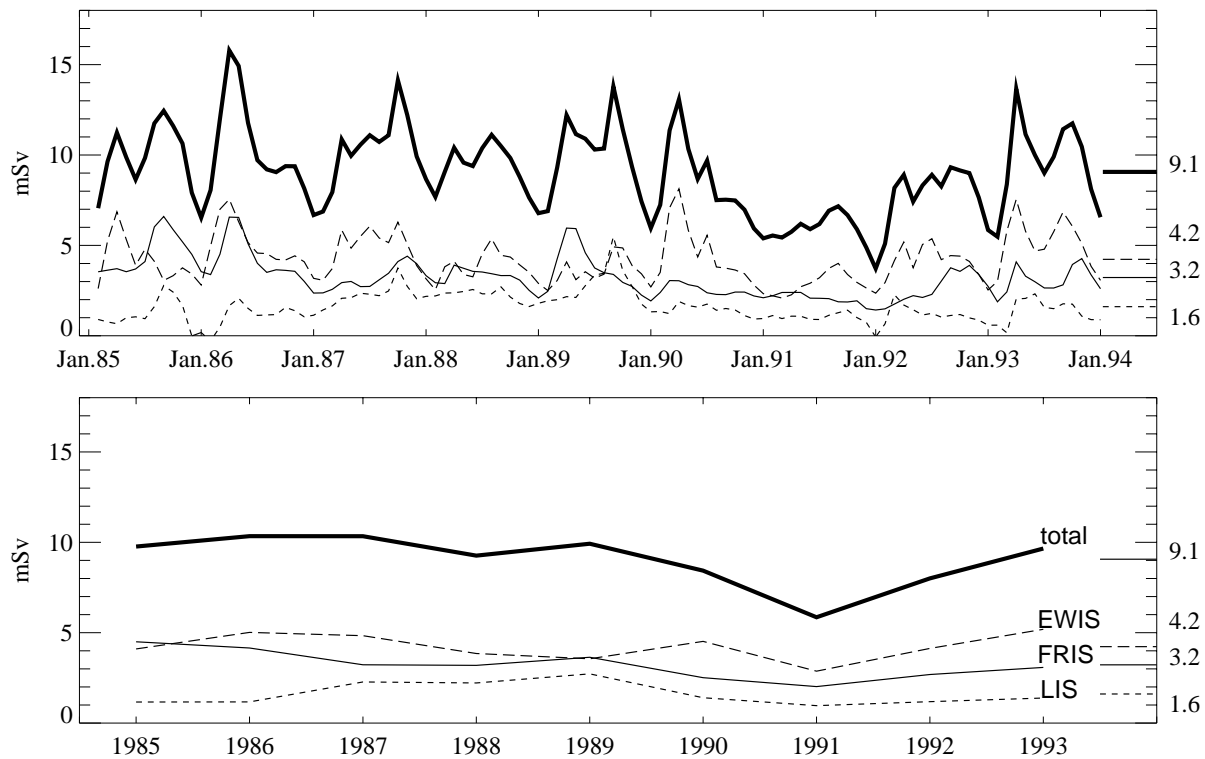


**Figure 10.** Time series of monthly (top) and annual (bottom) mean fresh water fluxes from total ice shelf melting (bold) and the contributions from FRIS (solid), EWIS (dashed) and LIS (dotted).